

THE USE OF DSC TO DETERMINE THE CURIE TEMPERATURE OF METALLIC GLASSES

A.L. GREER *

*Department of Metallurgy and Materials Science, University of Cambridge,
Cambridge CB2 3QZ (Gt. Britain)*

(Received 19 May 1980)

ABSTRACT

The subject of metallic glasses is introduced. These materials have technological potential, but only if their stability is adequate. It is, therefore, important to study their transformations on annealing, especially structural relaxation. The ferromagnetic Curie temperature, T_c , is a particularly useful parameter for monitoring structural relaxation and it can be measured by differential scanning calorimetry (DSC). The DSC method is convenient and accurate if temperature lags are corrected for. Ways of performing this correction in the DuPont DSC system are reviewed and a new method is proposed and tested. The experimental details of determining the T_c of metallic glasses are given. Finally, the relaxation behaviour of $Fe_{80}B_{20}$ glass, as studied by measuring its T_c , is reviewed. This behaviour is similar to that of conventional oxide glasses.

1. INTRODUCTION

Rapid quenching of molten alloys has been a subject of much scientific and technological interest for some time [1,2]. In addition to refined grain size, extended solid solubility and new metastable phases in crystalline products, it can produce non-crystalline phases. Non-crystalline alloys can be produced by a variety of other techniques, including vapour deposition, ion implantation, electrodeposition and chemical deposition, but we shall be concerned only with those produced by rapid quenching from the melt. When produced in this way the non-crystalline (or *amorphous*) alloys are perhaps best called *metallic glasses* [3] by analogy with conventional glasses. Several techniques have been used to achieve the rapid quenching. The basis of each is that a thin layer of liquid is formed in good thermal contact with a good conductor. Most interest has been shown in those methods which can produce a continuous product. In *roller-quenching* [4], a molten jet of alloy

* Present address: Division of Applied Sciences, Harvard University, Cambridge, MA 02138, U.S.A.

is projected between rapidly rotating rollers. In *melt-spinning*, the jet is projected on to the sloping inner surface or the flat outer surface of a rapidly rotating drum [5–7]. The most common method is melt-spinning, which can produce a continuous ribbon of constant cross-section (typically 50 μm thick and up to several millimeters in width) with uniform structure and properties. The cooling rate is of the order of 10^6C s^{-1} and the need to achieve this rate limits the thickness of ribbon, although Pd–Cu–Si glass [8] can be produced at a rate as low as 10^2C s^{-1} .

Even such a high cooling rate sets severe restrictions on the alloy compositions which can be obtained in non-crystalline form. Those which have been successfully quenched [9,10] fall into two main classes.

(a) Alloys of the late transition metals or noble metals and metalloids. The metals used include Au, Co, Fe, Mn, Mo, Ni, Pd and Ru. The metalloids used include B, C, Ge, P and Si. Typically, these glasses can be produced when the total metalloid content is 15–25 at.%.

(b) Alloys containing only metal atoms. These have now been produced in great variety, e.g. Cu–Zr, Nb–Ni, Ni–Ti, Ca–Mg, Mg–Zn, (Ti, Zr)–Be, U–Cr. Typically, the composition range over which these glasses can be produced is wider than in class (a), e.g. Cu–Zr can be quenched to a non-crystalline form in the range 25–60 at.% Cu [11].

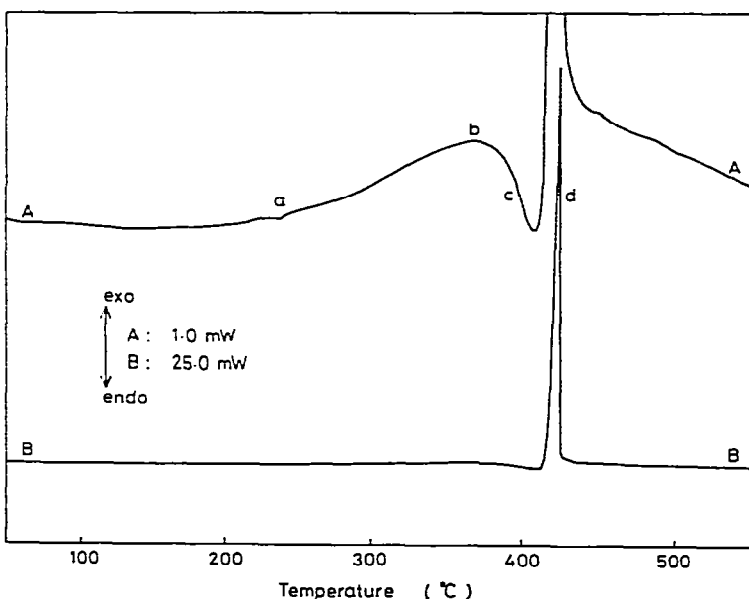


Fig. 1. DSC curves at different sensitivities obtained on heating a 4 mg sample of the amorphous alloy Metglas 2826 at 20C min^{-1} . The Curie transition is at point a. An exothermic reaction associated with the relaxation of the glass gives rise to the broad peak at b. The glass transition is at c, and the major peak at d shows the heat evolution as the glass crystallises.

The structure of metallic glasses has been studied by X-ray and neutron scattering [12]. It appears that they are truly non-crystalline and not micro-crystalline. The most successful model of the structure has been that based on the dense random packing of hard spheres [13], although models based on a more rigidly defined short range order may also be important [14].

Metallic glasses have interesting and some potentially useful properties, including mechanical strength [15,16] and corrosion resistance [17]. The alloys with the greatest potential, however, are those of the transition-metal metalloid type with a large fraction of iron (typical compositions in at. %: $\text{Fe}_{80}\text{B}_{20}$ and $\text{Fe}_{40}\text{Ni}_{40}\text{P}_{14}\text{B}_6$). These alloys are ferromagnetic [18] and their soft magnetic properties make them attractive for a number of applications [19]. They are the most widely studied type of metallic glass and the present work is restricted to this type.

The stability of metallic glasses has been extensively studied [20]. They are metastable, not only with respect to crystalline phases, to which they transform when the atomic mobility becomes high enough on heating, but also with respect to more "relaxed" glassy states. *Structural relaxation*, which can occur at times and temperatures far lower than those necessary for crystallisation, will, in principle, affect all the properties of metallic glasses. The Curie temperature of ferromagnetic glasses, being sensitive to relaxation and convenient to measure, is the property of immediate interest.

The transformations of metallic glasses may be studied using DSC. Figure 1 shows DSC curves for $\text{Fe}_{40}\text{Ni}_{40}\text{P}_{14}\text{B}_6$ glass obtained by heating at $20^\circ\text{C min}^{-1}$. This material is ferromagnetic and its Curie point at 235°C is visible on the more sensitive curve. (The attribution of such a feature to the Curie transition can be confirmed by magnetic measurements e.g. as in Fig. 13.) Between 250 and 400°C , there is a broad peak: this corresponds to an exothermic, irreversible reaction associated with the structural relaxation of the glass. At 390°C there is a sharp drop in specific heat attributed to the glass transition. (This was confirmed by dynamic mechanical analysis [21], which showed there was a peak in mechanical damping at the same temperature.) Shortly after the glass transition, the material crystallises and this exothermic reaction gives rise to the major DSC peak. Transmission electron microscopy and DSC have proved useful in determining the reaction kinetics [22,23]. That so much information can be obtained even from one DSC run illustrates the importance of this technique. The present concern, though, is just the use of DSC to determine Curie temperatures.

Metallic glasses will find technological application only if their stability is adequate. Crystallisation seems unlikely to be a problem, but structural relaxation may be significant under service conditions. In addition, the study of structural relaxation is important because it may offer possibilities for property optimisation. In subsequent sections, it will be shown that the Curie temperature, T_c , is a useful parameter in monitoring structural relaxation and that it can be measured using DSC. This can be a very accu-

rate method, but only when a temperature lag correction is carried out; a new means of doing so is presented. Finally, some results on $\text{Fe}_{80}\text{B}_{20}$ glass are given to illustrate the usefulness of the technique.

2. THE CURIE TRANSITION IN METALLIC GLASSES

Although much work has been done on the phase transition in pure ordered magnetic materials, it is only recently that the behaviour of disordered systems has been the subject of serious study [24]. Experimentally, this study has been advanced by the discovery that metallic glasses can be ferromagnetic: the fact that they can be made with high or low concentrations of magnetic atoms has enabled the effects of disorder and dilution on the Curie transition to be studied and theories of magnetism to be tested [18]. It was shown by Gubanov [25] that amorphous solids could be ferromagnetic; previously, it had been thought that the lack of long range atomic order would prohibit ferromagnetism. The effects of randomness on magnetic properties are far-reaching: some non-ferromagnetic crystals become ferromagnetic in their amorphous state [26], and in a particular metallic glass it has been shown [27] that the Curie temperature is higher than the glass transition temperature, i.e. that ferromagnetism can exist in the liquid state.

For metallic glasses, the sharpness of the Curie transition is dependent on the concentration of magnetic species (Fe, Ni, Co). Where that concentration is low, the transition is smeared (i.e. the magnetisation decreases slowly and smoothly to zero on heating), there is only a small specific heat anomaly associated with it [18], and the Curie temperature cannot be defined by conventional methods [28]. Annealing of such glasses causes the Curie transition to be still more smeared out [28]. While there is considerable scientific interest in these materials, which are close to the percolation threshold for a uniform ferromagnetic state [18], technological interest has centred on those metallic glasses having a high concentration of magnetic species (e.g. $\text{Fe}_{80}\text{B}_{20}$, $\text{Fe}_{40}\text{Ni}_{40}\text{P}_{14}\text{B}_6$) which are the subject of the present work.

The Curie transition in glassy alloys of the latter type has been studied by a.c. calorimetry [29] and has been shown to be sharp; indeed, it is very similar to that of a crystalline metal. This result is in agreement with theoretical predictions and enables T_c to be found by conventional magnetic measurements. Arajs et al. [30] have shown that for $\text{Fe}_{40}\text{Ni}_{40}\text{P}_{14}\text{B}_6$ (Metglas 2826: Allied Chemical Corp.), the kink-point method [31] and Arrott plots give the same value for T_c . Majumdar [32] has obtained consistent values of the Curie temperature of $\text{Fe}_{78}\text{Mo}_2\text{B}_{20}$ (Metglas 2605A: Allied Chemical Corp.) by three methods: low-field susceptibility measurements, determination of the temperature at which the rate of change of magnetisation with temperature is a maximum, and the use of modified Arrott plots. Because the Curie

transition of metallic glasses having a high proportion of magnetic species is so sharp, T_c may be determined by detecting the specific heat anomaly at the Curie point using DSC [33].

It has been known for some time that the Curie temperature of these glasses rises on annealing [33,34] and this can be of significance in T_c determinations. In order to determine T_c , if extrapolation of magnetic data is to be avoided, the sample has to be heated to at least T_c . If T_c is sufficiently high, the heating necessary to perform the determination may have an annealing effect, causing the Curie temperature to rise. Different methods of determination require the sample to be held for different periods at elevated temperatures and so the results may be inconsistent if there is a significant annealing effect at those temperatures. For $\text{Fe}_{40}\text{Ni}_{40}\text{P}_{14}\text{B}_6$ [30], referred to above, the measurements were consistent because the methods of determination involved the same thermal treatment of the sample. In the case of $\text{Fe}_{78}\text{Mo}_2\text{B}_{20}$ [32], the Curie point is below the temperature range for a significant annealing effect during the course of the determination. Thus, Majumdar obtained consistent results by different methods, as noted above. Furthermore, his value for the T_c of the as-received alloy as derived from magnetic measurements is 283°C , in excellent agreement with the value of 282.6°C obtained by DSC in the present work (Table 1, Sect. 3.5), demonstrating the validity of the DSC method. In the case of $\text{Fe}_{80}\text{B}_{20}$ glass, the Curie temperature (358.5°C) is sufficiently high for there to be a measurable annealing effect during a Curie point determination. The problems posed by this are discussed in Sect. 3.5, but for the moment it is important to note a particular advantage of the DSC method, viz. that, of the available methods for determining T_c , DSC is the most rapid and therefore the one which minimises the undesirable annealing effect.

3. THE MEASUREMENT OF CURIE TEMPERATURES BY DSC

The DuPont DSC system has been used throughout the present work. In Sect. 3.1, the system and its operation are described as a background to Sect. 3.2 and 3.3 in which are presented a model for the heat flow in the system and a new method of correcting for the temperature lag on heating based on the model. The use of DSC to determine Curie temperatures is then described, first for a conventional crystalline material, nickel, and subsequently for metallic glasses.

3.1. The DuPont DSC system

The DSC system manufactured by E.I. DuPont de Nemours and Co., Inc. is of the heat-flux type and the principle of its operation has been described by Baxter [35]. The temperature difference between the sample and an inert reference (usually an empty sample pan and lid) is measured and, because

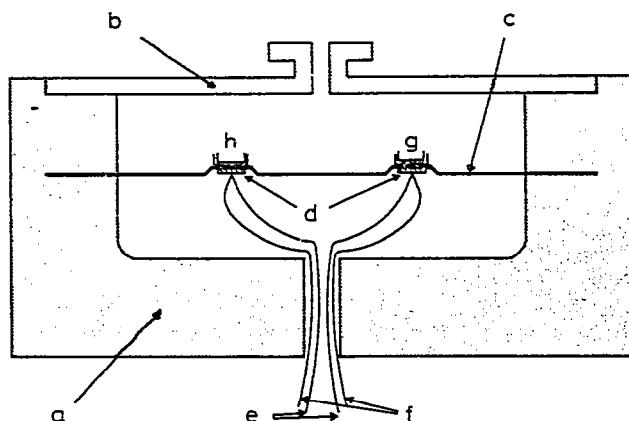


Fig. 2. A cross-sectional view of the DuPont DSC cell. a, Silver heating block; b, lid; c, constantan disc; d, chromel discs; e, chromel wires; f, alumel wires; g, pan and lid containing sample; h, reference pan and lid.

the thermocouples measuring this differential temperature are removed for the sample and reference, the differential heat flow is proportional to the differential temperature. Another result of the separation of thermocouple and sample is that the temperature of the sample lags behind that of the thermocouple on continuous heating and Sect. 3.3 describes how this may be compensated for. The DSC cell is illustrated in Fig. 2. It consists of a furnace and silver heating block, the block having inside it a cylindrical chamber containing a constantan disc. The disc has two raised platforms on which the sample and reference holders are placed. A chromel disc and connecting wire are attached under each platform and these two chromel-constantan thermocouples measure the differential temperature. In addition, an alumel wire is attached to each chromel disc and, on the sample side, the chromel-alumel thermocouple thus formed is used to measure the sample temperature. A thermocouple embedded in the silver block is connected to a proportional controller so that the temperature of the block can be programmed.

It is normal to use an inert purge gas in the cell to prevent oxidation of the constantan disc. In the present work, argon was used at a flow rate of 40 ml min^{-1} at ambient pressure. The quality of the DSC curve is very sensitive to fluctuations in the flow rate. A two-stage regulator, followed by a large diaphragm constant pressure stage and a Penning valve, enabled the flow rate to be controlled to better than $\pm 1 \text{ ml min}^{-1}$ over long periods of time.

The DuPont DSC system used here consisted of two components, the model 910 calorimeter and the model 990 console. The 910 unit contains the DSC cell itself, as described above, and a base module which performs several important functions: it provides reference junction compensation for the thermocouples, linearises the output of the furnace control thermo-

couple for proper temperature programming, and allows control of the baseline slope. In addition, the unit allows the choice of two amplification modes for the differential temperature (ΔT) signal before going to the recorder. In the "normal" mode, a constant amplification of 3000 is used. The recorder deflection can then be converted to millivolts and so ΔT may be obtained directly. This mode is useful when ΔT and the actual temperatures of various parts of the cell are to be determined, as in Sects. 3.2 and 3.3, but, in ordinary use, it is inconvenient because the thermal resistances in the cell which determine the sensitivity vary significantly with temperature. In the "calibrated" mode, the amplification is automatically varied with temperature to give a nearly constant calorimetric sensitivity.

Another point to be made about the determination of ΔT from the recorder is that the signal should be measured relative to the pen position when ΔT is zero, i.e. when there are no temperature gradients in the cell. In general, the position of the pen when this is true does not correspond with the electrical zero position when the input is short-circuited. Accordingly, it is necessary to find the pen position when ΔT is zero by allowing the cell to equilibrate at ambient temperature. This position, at a given sensitivity, will be a fixed distance from the electrical zero position. Correction by this distance enables ΔT to be determined from the pen position relative to the electrical zero, a convenient procedure in practice.

The other component of the DuPont DSC system, the 990 console, contains the temperature programmer and the recorder. In the present work, the programmer was used to increase temperature linearly with time. The recorder has two pens. Sample temperature was recorded on the abscissa and both pens recorded the differential temperature signal (at different sensitivities) on the ordinate.

3.2 *A model for the heat flow*

A description of the heat flow in the DuPont DSC cell can be attempted by assuming that the heat flow rate between two points is proportional to the temperature difference between those points, i.e. a thermal Ohm's Law. The following treatment is based on that of Baxter [35], but, because there are some ambiguities in his description, the terminology has been altered. Firstly, the following quantities are defined.

$T_S(^{\circ}\text{C})$ sample temperature, i.e. the temperature of the sample and its container

This temperature is assumed to be uniform throughout the sample and its container. The validity of this assumption will be discussed in the next section.

$T_R(^{\circ}\text{C})$ reference temperature, i.e. the temperature of the reference pan and lid (and of the reference material, if any)

$T_{SP}(^{\circ}\text{C})$ temperature of the sample platform
 This is taken to be the temperature of the chromel—constantan and chromel—alumel thermocouples at that point. In normal use, it is read off the abscissa of the recorder as the sample temperature.

$T_{RP}(^{\circ}\text{C})$ temperature of the reference platform, taken to be the temperature of the chromel—constantan thermocouple at that point

$T_F(^{\circ}\text{C})$ furnace temperature as set by the programmer, i.e. the temperature of the silver heating block to which the constantan disc is attached

$R_D(^{\circ}\text{C min J}^{-1})$ thermal resistance between the furnace wall and the sample or reference platforms

The heat flow to the two platforms is assumed to be independent. The heat flow is mainly through the constantan disc, but some flow takes place through the gas in the chamber. The resistance is reproducible, provided the gas flow is kept constant. R_D varies with temperature.

$R_S(^{\circ}\text{C min J}^{-1})$ thermal resistance between the sample platform and the sample

This resistance has several components: the contact resistance between the constantan disc and the sample pan, the resistance of the sample pan, the contact resistance between the pan and the sample, and the resistance within the sample. These will be discussed more fully in Sect. 3.3 where it will be shown that, for small samples, it is convenient and appropriate to assume that the first three components are reproducible and that the last is negligible.

$R_R(^{\circ}\text{C min}^{-1} \text{J}^{-1})$ the equivalent of R_S for the reference

$C_S(\text{J } ^{\circ}\text{C}^{-1})$ heat capacity of the sample and its container

$C_R(\text{J } ^{\circ}\text{C}^{-1})$ heat capacity of the reference and its container

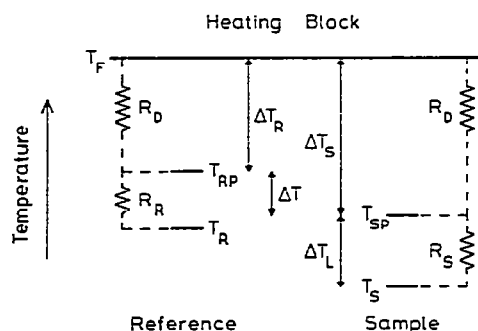


Fig. 3. Schematic temperature distribution in the DuPont DSC cell. The broken lines show the thermal resistances between the points at which the temperatures are measured.

$H(^{\circ}\text{C min}^{-1})$ heating rate, i.e. the rate of temperature increase of the heating block

When the cell is heated at a uniform rate, a dynamic equilibrium is soon established in which all parts have the same rate of temperature increase, but are at different temperatures. These temperature differences drive the heat flow in the cell and are illustrated schematically in Fig. 3. The following are of interest.

ΔT_R temperature lag of the reference platform behind the furnace
 ΔT_S temperature lag of the sample platform behind the furnace
 ΔT differential temperature signal, which in normal use is plotted on the ordinate on the recorder

ΔT_L temperature lag of the sample behind the sample thermocouple

The following equations then hold.

$$\Delta T_R = HR_D C_R \quad (1)$$

$$\Delta T_S = HR_D C_S \quad (2)$$

$$\Delta T = HR_D (C_S - C_R) \quad (3)$$

$$\Delta T_L = HR_S C_S \quad (4)$$

$$\Delta T_S = \Delta T_R + \Delta T \quad (5)$$

$$\Delta T_L = (R_S/R_D) \Delta T_S \quad (6)$$

A most important point, though, is that the thermal resistances, R_S , R_R and R_D , and the capacities, C_S and C_R , can vary with temperature. It has been assumed that on heating at a uniform rate, a steady state is established: this will not be true if the thermal resistances or heat capacities change sharply and, in that case, eqns. (1)–(6) will be only approximately true. In general, though, these quantities do not undergo abrupt changes and the equations are expected to be valid.

Before using eqns. (1)–(6) to correct for the temperature lag, ΔT_L , it is desirable to test the model. A number of experiments was conducted to this end and their results are described below. In these tests, it was valid to assume that the thermal resistances and heat capacities were constant (though it is not true in general), because the results were all taken with the cell temperatures close to the Curie point of nickel.

If a given inert (i.e. non-reacting) sample is heated against the same reference at different heating rates, eqn. (3) predicts that the differential temperature signal at any temperature should be proportional to the heating rate, H , (R_D , C_S and C_R being constant). A sample of nickel was heated at various rates and the value of ΔT at one temperature, the Curie temperature (see Sect. 3.4) determined from the recorder. The results are shown in Fig. 4: the value of ΔT is proportional to the heating rate. A further test was performed at the same time. The values of the Curie temperature of the nickel,

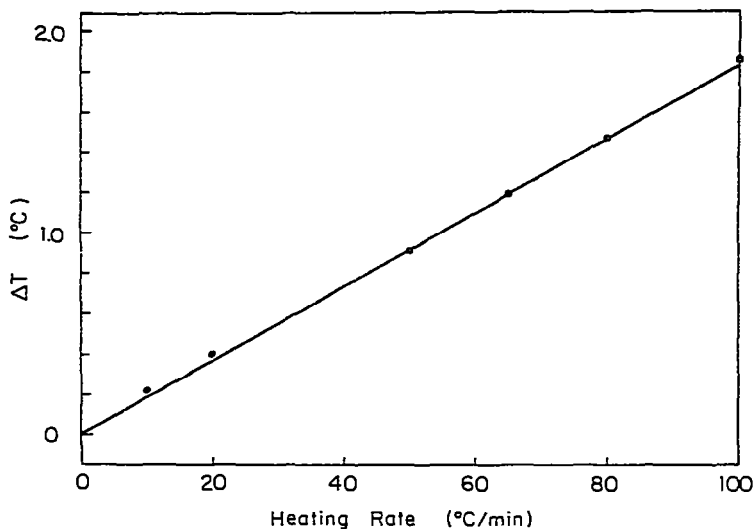


Fig. 4. The variation of the temperature difference between the sample and reference platforms, ΔT , with heating rate for a 37.8 mg sample of nickel. The reference was an empty pan and lid. ΔT was measured at the Curie temperature of the nickel.

as read on the abscissa of the recorder (i.e. T_{SP} values), were recorded and they are displayed in Fig. 5 as a function of the heating rate. The measured Curie temperature rises linearly with heating rate. Assuming that the actual temperature of the Curie transition is unaffected by the heating rate, this lin-

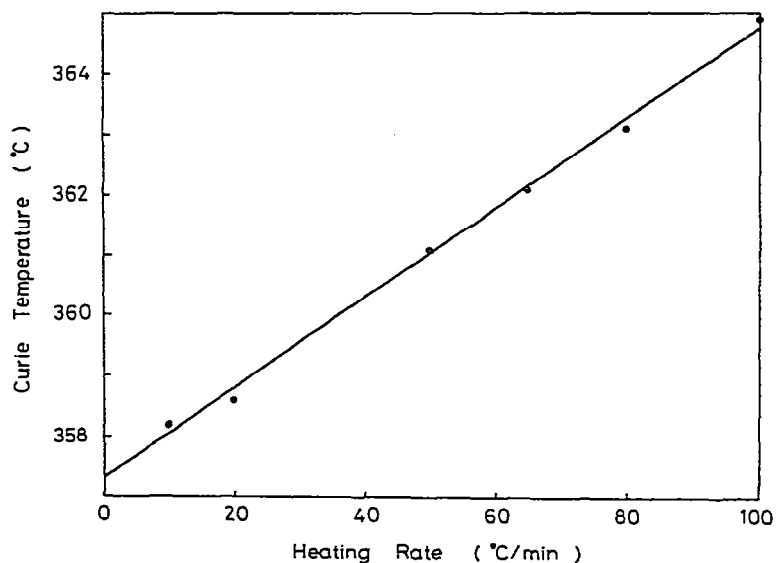


Fig. 5. The variation of the measured Curie temperature of a 37.8 mg sample of nickel as a function of heating rate. The apparent Curie temperature rises because the temperature lag of the sample behind the sample platform increases linearly with heating rate.

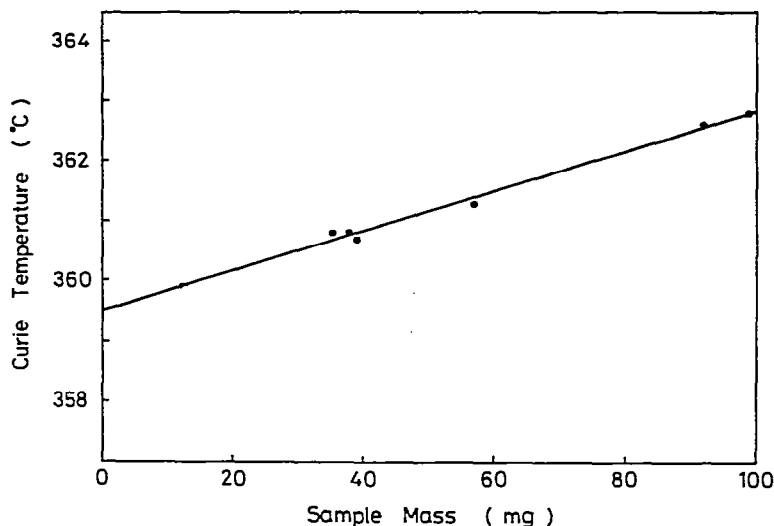


Fig. 6. The variation of the Curie temperature, measured at a heating rate of $50^{\circ}\text{C min}^{-1}$, of samples of nickel as a function of their mass. The apparent Curie temperature rises because the temperature lag of the sample behind the sample platform increases linearly with sample mass.

ear increase reflects a linear increase in the sample temperature lag, ΔT_L , with heating rate as predicted by eqn. (4) (R_S and C_S being constant). Different samples of nickel were heated at the same rate ($H = 50^{\circ}\text{C min}^{-1}$) and the apparent Curie temperature read on the recorder as before. These values are shown in Fig. 6 as a function of the sample mass. Again, the values rise linearly as would be expected from eqn. (4); the heat capacity, C_S , will rise linearly with sample mass and the other two quantities in the equation, H and R_S , are constant. Together, these tests strongly support the proposed model and its underlying assumption of a thermal Ohm's law. The model neglects the heat capacities in the cell, except those of the sample and reference, but this simplification does not seem to present any problem.

3.3 Correction for temperature lag

It has been shown above that the sample temperature lags by an amount ΔT_L behind that of the thermocouple on the sample platform. Some methods proposed for the correction of this lag are summarised below and then a new method, developed for the present work, is proposed and evaluated.

Existing methods

The temperature lag is proportional to heating rate, viz.

$$\Delta T_L = HR_S C_S \quad (4)$$

If a sample undergoes a transition at a temperature which is independent

of heating rate, then its apparent transition temperature may be plotted as a function of heating rate, and extrapolation to zero heating rate gives the true value of the transition temperature. The results of such an experiment, measuring the Curie temperature of a 37.8 mg sample of nickel, have already been presented in Fig. 5. From the plot, the value of the temperature lag for that sample at any heating rate may easily be found and it can be seen that the variation is indeed linear. This is one way of correcting for the temperature lag: the same sample, if it is unaffected by the repeated heating, is heated at various rates and the true value of the transition temperature found by extrapolation. If the sample is affected by heating through the transition, a new sample must be used each time; in this case, all the samples must be of the same mass, since ΔT_L is proportional to the heat capacity of the sample. Such a method is inconvenient, requiring several runs for each determination. Nevertheless, it may be used to derive the temperature lag for one sample of a given mass. This lag may then be assumed to apply to a series of samples [36] if these are of similar materials and closely matched in mass (i.e. of constant C_S). The disadvantage of the method is that there is no independent measurement of the lag for each sample.

Furthermore, the initial determination of the lag is valid only if the transition temperature is independent of heating rate. Even when this is not the case, the true value of the transition temperature can be found. Samples of various masses are heated at the same rate and the apparent values of the transition temperature plotted as a function of C_S . Again, the plot will be linear and, this time, extrapolation is made to zero C_S . This method also suffers from the disadvantage of having to perform several runs in order to get one value of the transition temperature. In addition, C_S has to be determined for each sample. It should be noted that C_S includes the heat capacity of the sample pan and therefore an extrapolation to zero sample mass, as in Fig. 6, is not sufficient to determine the transition temperature.

The problems described above are overcome in the method of Barton [37]. After heating through the region of interest, the instrument is switched to the isothermal mode and the ΔT transient while the sample and reference attain the same final temperature is plotted with time on the abscissa. The area under this transient is measured, rather as the area under a DSC peak, to give the total heat necessary to equilibrate the cell temperature. Knowing the heat capacities of the sample and reference, the temperature lag can be derived. This method is generally applicable and has the great advantage that the lag is derived for each sample. It does, however, require simultaneous recording of time, temperature (i.e. T_{SP}) and heat flow (i.e. ΔT) data. Barton [37] achieves this by attaching the DuPont 990 console to a digital voltmeter, data transfer unit and paper tape punch, but it is not possible with the standard DuPont system. Furthermore, the Barton method requires a fair degree of calculation to work out the lag in each case.

A new method

A new method for correcting the temperature lags in the DuPont DSC system is presented here. It is not generally applicable, but was devised for, and is particularly suited to, the case of metallic glass Curie temperature measurements, where a large number of runs has to be performed on samples of small mass. For such a case, it is more convenient than the Barton method, which requires the measurement of an area on the curve for each run and, in addition, it is possible with the standard DuPont DSC system with two-pen chart recorder. It will be shown below that Curie temperature measurements are reproducible to $\pm 0.2^\circ\text{C}$ (S.D.). In order to have similar reproducibility in the corrected values the method of correction must be accurate. The proposed method gives the required accuracy, without weighing the samples, which would be necessary to obtain similar accuracy by the Saffell [36] method.

As shown earlier, the temperature lag of the sample, ΔT_L , is given by

$$\Delta T_L = (R_S/R_D) \Delta T_S \quad (6)$$

At any particular temperature (and, to a good approximation, over a small range of temperature), the resistance of the constantan disc, R_D , is constant and, assuming that R_S is also constant and can be found by experiment, ΔT_L can be derived from ΔT_S . It has been shown that the temperature lag of the sample platform behind the furnace, ΔT_S , is given by

$$\Delta T_S = \Delta T_R + \Delta T \quad (5)$$

ΔT_R is the temperature lag of the reference platform behind the furnace and is independent of the sample. It depends on the reference and is proportional to the heating rate. ΔT is just the differential temperature signal which is measured in any case.

Thus the temperature lag may be calculated if R_S/R_D and ΔT_R for a given reference and at any heating rate are known. During the heating run on a sample, ΔT is measured and using eqns. (5) and (6) in turn yields ΔT_S and ΔT_L . These relationships may be made clearer by reference to Fig. 3.

In applying this method of correction, it is appropriate to operate the instrument with the temperature on the recorder abscissa and both pens showing the ΔT signal. One pen operates at high sensitivity to record the DSC curve in detail and enable accurate measurement of the transformation temperature. The other pen is set at a low enough sensitivity that its full deflection from the zero signal position is on scale. From this second pen, the magnitude of ΔT can be determined at any temperature, as described in Sect. 3.1. It is appropriate to measure ΔT at the transformation temperature.

ΔT_R is measured for a particular reference, usually just an empty pan and lid. First of all, a heating run is performed with an empty pan on both sample and reference platforms. Then the chosen reference is placed in the *sample*

pan and the run repeated at the same rate. The ordinate distance between the two DSC curves at any temperature is ΔT_R at that temperature and heating rate. [This may be derived from eqns. (1) and (3).] The experiment is repeated to determine ΔT_R at different heating rates.

Addition of ΔT and ΔT_R , determined as above, gives ΔT_S . Figure 7 shows the values of ΔT_S at the Curie temperature of a 37.8 mg sample of nickel heated at various rates. The plot is linear as expected from eqn. (2). Other results from the same heating runs have been plotted in Figs. 4 and 5, the latter showing the variation of measured Curie temperature with heating rate. The ratio of the gradients in Figs. 5 and 7 gives the ratio R_S/R_D for this sample.

The sample used in these heating runs was a disc, 0.245 mm thick, cut from a 5 mm diameter rod of nickel (from Johnson Matthey Chemicals Limited; details of composition are given in the Appendix). A series of discs of different thicknesses was cut from the rod. The results from runs in which these discs were heated at $50^\circ\text{C min}^{-1}$ have already been presented in Fig. 6. For each sample, the variation of apparent Curie temperature and ΔT_S with heating rate were measured and R_S/R_D determined. A straight line was fitted, using the least squares method, to each plot of Curie temperature against heating rate and the true value estimated by extrapolation to zero heating rate. The estimated values of true Curie temperature and R_S/R_D for these samples are plotted as a function of sample thickness in Fig. 8. The implications are discussed below.

The thermal resistance, R_S , between the sample platform and the sample has a number of components, viz.

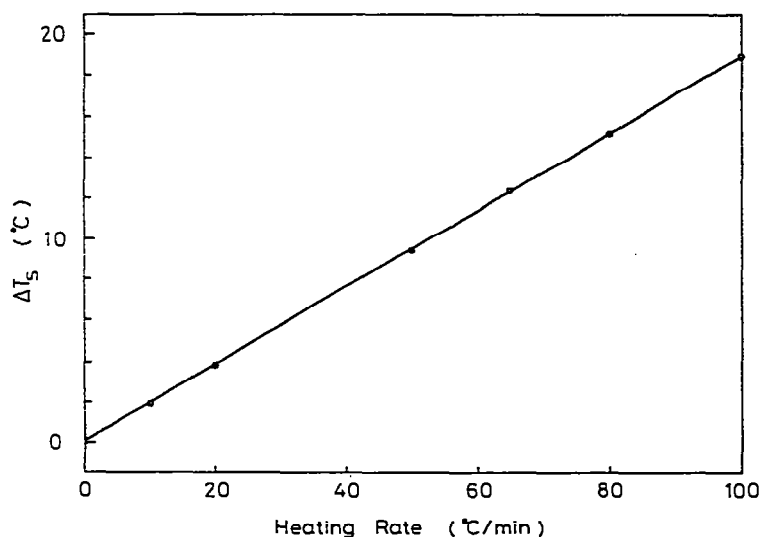


Fig. 7. Variation with heating rate of the temperature lag of the sample platform behind the heating block, ΔT_S , for a 37.8 mg sample of nickel at its Curie temperature.

- (a) the contact resistance between the constantan disc and the sample pan,
- (b) the resistance of the sample pan,
- (c) the contact resistance between the pan and the sample, and
- (d) the thermal resistance within the sample.

When the same nickel sample is heated several times, the reproducibility of the Curie temperature is very good (Sect. 3.4) despite replacing the sample pan on the platform between the runs. In this case, components (b)–(d) are constant, so the reproducibility must mean that component (a) is constant. It is, though, expected to vary over a long time as the constantan disc ages and oxidises [36]. This will also affect the resistance of the disc itself. Component (b) is constant. For a series of samples such as described above, component (c) is expected to be constant, while component (d) will vary with sample thickness. The average temperature lag in a thick sample is proportional to the square of the thickness, so that the effective R_S will rise more than linearly with thickness, as shown in Fig. 8. As the thickness tends to very small values, component (d) is expected to become negligible and the sample can be assumed to be at uniform temperature.

The variation of estimated “true” Curie temperature (Fig. 8) is of concern. The Curie transition of a thick sample may register on the DSC curve before the average temperature of the sample has reached the Curie temperature, T_c ; i.e. the DSC curve is distorted. In this case, when the measured Curie temperature is plotted against heating rate, the values of T_c at the higher heating rates will be lower than predicted from the linear relation [eqn. (4)]. Fitting a straight line, by least squares method, will give an unduly high intercept, i.e. extrapolated value of T_c at zero heating rate. Fortunately, this effect becomes negligible at low thicknesses (<0.4 mm).

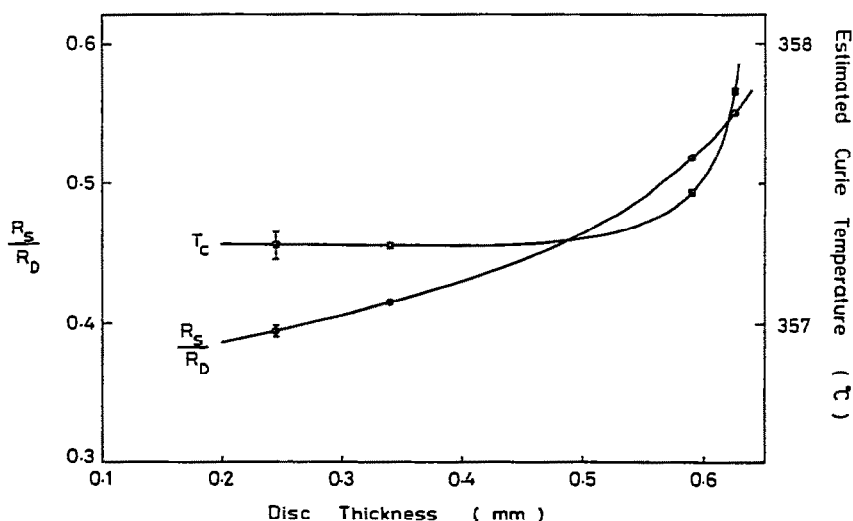


Fig. 8. Estimated values of Curie temperature and R_S/R_D at the Curie temperature for nickel discs, 5 mm in diameter, as a function of disc thickness.

Thus the model outlined in Sect. 3.2 will work for sufficiently thin samples and, where R_S/R_D can be taken to be constant, the method for correcting temperature lag can easily be applied. R_S/R_D can be constant only in a small temperature range and then only if R_S is reproducible. The component of R_S most likely to lead to variation is the thermal resistance in the sample. If, however, the samples lie flat on the bottom of the sample pan, are of the same uniform thickness and have the same thermal conductivity, this component will be constant. Or, if the samples are very thin and are good thermal conductors, this component, though varying, may be so small as to be negligible. The conditions for R_S to be constant may appear stringent, but in practice they may often be met for a series of samples whose thermal characteristics are to be compared. For example, the metallic glass samples of interest in the present work are of uniform thickness and thermal conductivity. Furthermore, the thickness ($\sim 40 \mu\text{m}$) is low and the thermal conductivity is good, with the result that temperature gradients in the sample are probably negligible.

In conclusion, the proposed method for correcting temperature lags has some advantages. The samples do not need to be weighed; although the lag is proportional to the sample mass, the method determines the lag individually for each sample. The model developed in Sect. 3.2 showed that the temperature difference between sample and reference platforms is related to the temperature lag through eqns. (5) and (6). Once R_S/R_D and ΔT_R have been determined, the ΔT signal, which is the signal normally recorded on DSC curves, can be used to calculate the temperature lag of the sample behind the sample thermocouple. This method is quick and convenient, but caution must be exercised since it depends on R_S/R_D being constant. If the sample masses vary widely, R_S may not be constant and, in any case, all the thermal resistances vary with temperature, so that the method is valid over only a limited range of temperature. Nevertheless, the method presented here can be applied with success to the measurement of the Curie temperatures of metallic glasses (Sect. 3.5). These measurements require accurate temperature determination, but only over a small range ($< 20^\circ\text{C}$) and R_S/R_D is determined at a temperature in about the middle of the range. The lag in Curie temperature determinations is typically $2\text{--}3^\circ\text{C}$; it is, therefore, important to take it into account in measurements which are reproducible to $\pm 0.2^\circ\text{C}$.

3.4 The Curie transition of nickel

As the temperature is raised, the magnetisation of a ferromagnetic material decreases more and more rapidly, reaching its maximum rate of fall at the Curie temperature, T_c , where it drops almost to zero. This sharp drop at the Curie point may be used to determine the Curie temperature, or more sophisticated treatments of the magnetic data may be employed [38]. The changes in energy accompanying the changes in spontaneous magnetisation

give rise to a specific heat anomaly around the Curie point and, for this reason, calorimetry can be used to study the Curie transition. Superimposed on the normal variation of specific heat with increasing temperature is a cusp, the specific heat increasing to a maximum at T_c and dropping sharply above it. This is shown for crystalline nickel in Fig. 9 where the data from conventional calorimetry [39] and DSC (present work) are compared. It can be seen that there is some systematic error in the calorimetric calibration of the instrument (performed by measuring the specific heat of sapphire).

To determine the Curie temperature by DSC, it is not necessary to perform a calorimetric calibration and derive the specific heat; it is easily determined directly from the DSC curve. Figure 10 shows DSC curves for nickel obtained on heating at $10^\circ\text{C min}^{-1}$ and $100^\circ\text{C min}^{-1}$. In one case, the sharp peak at a is taken to indicate T_c ; in the other case, T_c is determined by extrapolation. Compared with most transitions, the width of the Curie transition is relatively unaffected by the heating rate. At high heating rates, or for large samples, there is a slight broadening as in Fig. 10, but this is believed to be due to the temperature gradient in the sample rather than a fundamental broadening of the transition. Norem et al. [40] have reported thermogravimetric results showing that, for their samples, which were in a low magnetic field, there was some supercooling of the Curie transition, but no superheating. For this reason, the Curie temperatures in this work, where the samples are in an effectively zero magnetic field, have been measured on heating.

Using DSC ($H = 50^\circ\text{C min}^{-1}$), eight Curie temperature determinations were carried out on one sample of nickel (5 mm diameter disc, 0.245 mm thick).

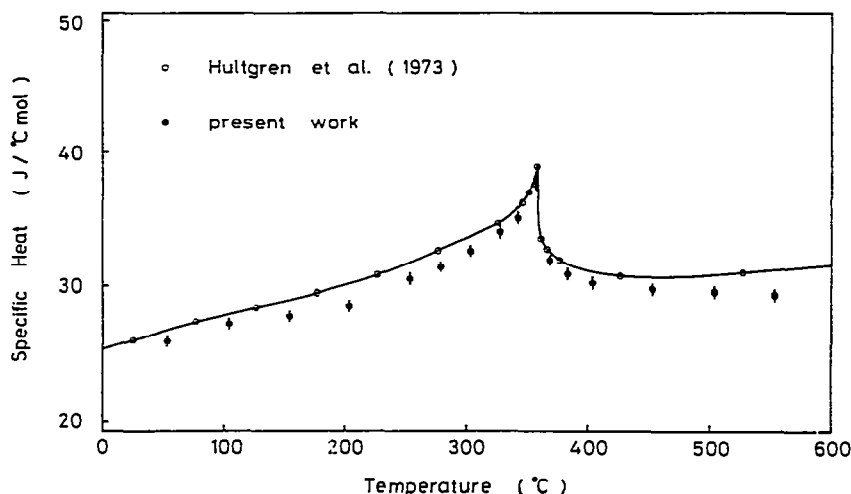


Fig. 9. The specific heat of pure crystalline nickel near its Curie point. The data from conventional calorimetry [39] and DSC (present work) are compared.

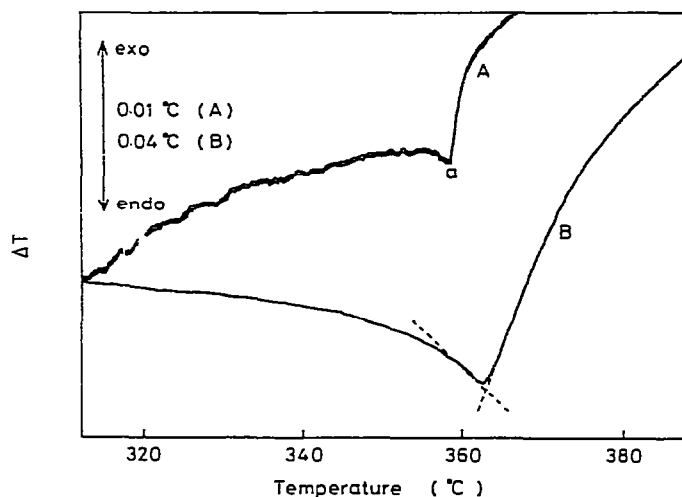


Fig. 10. DSC curves obtained on heating an 8.90 mg sample of nickel sponge (composition in Appendix): A, at $10^{\circ}\text{C min}^{-1}$; B, at $100^{\circ}\text{C min}^{-1}$. On slow heating, the Curie point is well defined, as at a. On fast heating, the transition is blurred, but the Curie point can still be determined accurately by extrapolation.

Different sample pans and lids were used for each determination; thus the reproducibility, not only of the transition, but also of the thermal resistances in the cell was tested. The standard deviation of the eight values was 0.14°C . This excellent reproducibility, together with the ease of identification of the transition temperature, makes the Curie point of nickel useful for calibration. It is particularly useful in calibrating thermogravimetric apparatus where, in a magnetic field, the apparent weight change of the sample, associated with the transition, can be detected [40].

The calibration, though, depends on knowing the Curie temperature of nickel and there is some uncertainty about this. The generally accepted value is 358°C , obtained by low-field magnetic measurements. Williams and Chamberland [41] point out that in DSC the determination is made in zero field. Citing the theoretical work of Arrott [38], they suggest that the correct value for the zero-field Curie temperature is 354°C . Norem et al. [40], however, show that for the fields used in their thermogravimetric apparatus the Curie temperature is independent of the field, but also suggest a value of 354°C . Nevertheless, in the present work, 358°C has been taken as the value of T_c ; determination by DSC is a zero-field calorimetric measurement and in conventional calorimetry with no magnetic field applied, the sharp maximum in the specific heat of nickel occurs at 358°C [39,42].

Further uncertainties can arise because the Curie temperature of nickel can vary with the nature of the sample. Sykes and Wilkinson [42] have shown that the effect of heat treatment on the sample (i.e. of the grain size) is negligible, but that the Curie point is very sensitive to the purity. For example, 1% of cobalt raises T_c by 12°C , 1% of silicon lowers it by 70°C ,

and an increase in iron content of 0.01% was enough to cause a 1°C drop. In the present work, three types of nickel were used, nickel sponge, nickel rod and carbonyl nickel pellets. The sources and composition of these are given in detail in the Appendix, but the order above is of decreasing purity. For each type of nickel, a small sample was taken and heated in the DSC at a number of rates. As described in Sect. 3.3, extrapolation to zero heating rate gives the true value of the Curie temperature. For the three types of nickel, the values of T_c (uncalibrated) thus determined were

nickel sponge	$360.2 \pm 0.15^\circ\text{C}$
nickel rod	$359.7 \pm 0.15^\circ\text{C}$
nickel pellet	$358.7 \pm 0.15^\circ\text{C}$

The differences in these values could be accounted for by the differences in purity. It was assumed that the value for the purest material, nickel sponge, was the most accurate, and the instrument was calibrated to make the Curie point of the nickel sponge read as 358°C.

This calibration was consistent with those obtained using the melting points of tin (231.9°C) and zinc (419.5°C). However, it should be noted that, with only two adjustments, it is not usually possible to obtain correct temperature readings over the whole temperature range of the instrument, especially with an aged thermocouple. Calibration must be carried out in the region of interest and nickel ($T_c = 358^\circ\text{C}$) is a particularly useful standard when studying T_c changes in $\text{Fe}_{80}\text{B}_{20}$ glass (as-quenched $T_c = 358.5^\circ\text{C}$). Calibration was carried out by adjusting the recorder until the specific heat cusp occurred at the correct temperature, the "correct temperature" not being T_c itself, but allowing for the temperature lag.

In conclusion, the study of nickel shows that DSC may be used to measure Curie temperatures. The absolute *accuracy* of the determination may not be high ($\pm 2.0^\circ\text{C}$), because of uncertainties in calibration, but the *precision* is very high ($\pm 0.14^\circ\text{C}$). This reproducibility makes the Curie transition of nickel itself useful for calibration when studying T_c changes in some metallic glasses.

3.5 Curie temperature determination for metallic glasses

The experimental details of T_c determination for the particular case of $\text{Fe}_{80}\text{B}_{20}$ glass are given below. These details are similar for a number of glasses and the T_c values of some of these are presented and discussed.

Figure 11 shows some DSC curves of the Curie transition in Metglas 2605 ($\text{Fe}_{80}\text{B}_{20}$): they are similar to that for nickel. For as-received material, some variability in the shape of the DSC cusp is observed, e.g. the difference between curves A and B in Fig. 11. This variability in shape did not, however, cause a large scatter in the values of T_c , which were determined using the tangent construction shown in Fig. 10. Annealed specimens (e.g. curve C in Fig. 11) always showed a sharp Curie transition and gave slightly more

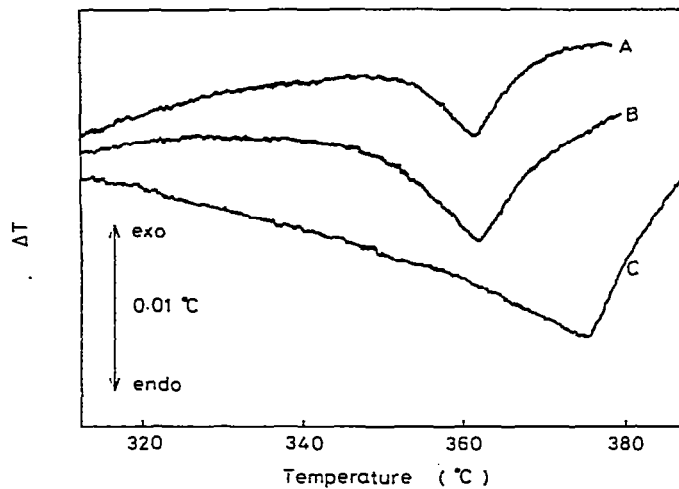


Fig. 11. DSC curves obtained on heating samples (~ 4 mg) of Metglas 2605 ($\text{Fe}_{80}\text{B}_{20}$) at $50^\circ\text{C min}^{-1}$ through the Curie transition. A, B, As-received; C, pre-annealed at 280°C for 24 h.

reproducible values of T_c . (The sharpening of Curie transition on annealing is probably due to stress relief, see below.) Note that the annealing causes T_c to rise. Metglas 2605 comes in the form of ribbon about $40\ \mu\text{m}$ thick and $1.0\ \text{mm}$ wide: it has a rough side and a smooth side. The samples for DSC were prepared as follows: three $\sim 5\ \text{mm}$ lengths were placed rough side up in the bottom of the sample pan; they were checked to make sure they did not overlap and a lid was put on top. The object of this procedure was to obtain good and reproducible thermal contact between the metallic glass and the sample pan. The effect of heating rate on the sharpness of the Curie transition on the DSC curve was the same as for nickel (Fig. 10). Because of the low sample mass, $\sim 4\ \text{mg}$, a fairly high heating rate of $50^\circ\text{C min}^{-1}$ was chosen; this gave a good signal-to-noise ratio without smearing the transition. The reproducibility of T_c values was not as good as for nickel: the standard deviation for as-received Metglas 2605 was 0.25°C , while for heat-treated samples it was 0.2°C . The increased scatter may be due to irregularities in the specimen geometry, while the reason for the difference in scatter between as-received and annealed samples is discussed later in this section.

Because of the annealing effect during a Curie point determination, the true Curie temperature is not the same at different heating rates. It is not possible to take a sample in any condition and heat it at various rates to determine the temperature lag and R_S/R_D as in Sect. 3.3. It is necessary to anneal several samples to a condition where T_c has stabilised and is unaffected by the annealing during the determination. An anneal of 10 min at 400°C was chosen for this purpose. These samples are then heated at different rates and the value of R_S/R_D determined as before. The plot of T_c

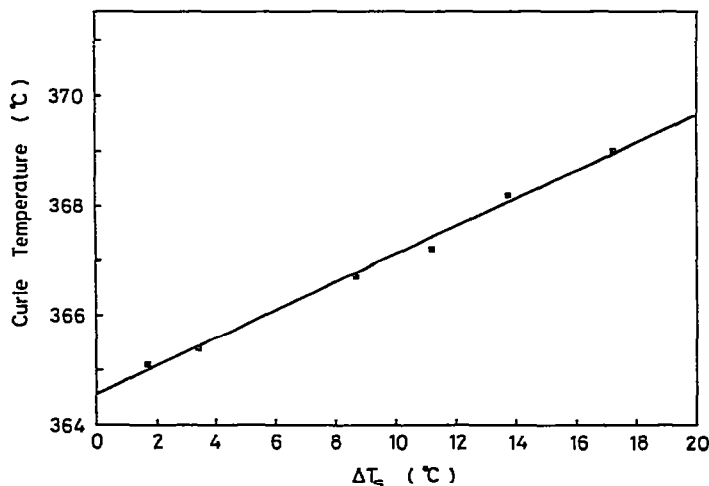


Fig. 12. The variation of Curie temperature, as determined from DSC curves without correcting for temperature lag, with ΔT_s for samples (~ 4 mg) of Metglas 2605 heated at 10, 20, 50, 65, 80 and $100^\circ\text{C min}^{-1}$. The gradient of the plot is R_S/R_D , which is needed to correct for the temperature lag. The samples have been pre-annealed at 400°C for 10 min to stabilise the Curie temperature.

vs. ΔT_s is given in Fig. 12. The value of R_S/R_D for Metglas 2605 samples prepared as above is 0.28. Using this value, the T_c determinations can be corrected for temperature lag and this correction has been carried out for all subsequent determinations in this work. The lag for a 4 mg sample heated at $50^\circ\text{C min}^{-1}$ is approximately 2.2°C , so it is important to take it into consideration.

Unlike nickel, it is normally desirable to make only one Curie point determination on a Metglas 2605 sample. The determination involves heating the sample to around 400°C , and not only does this have an effect on T_c itself, but it may partially crystallise the sample.

For a novel material like Metglas 2605, it was necessary to confirm that the effect shown in the DSC curves (Fig. 11) really is the Curie transition. The immediate evidence suggesting this is the shape of the DSC curve, which is similar to that at the Curie point of nickel. Furthermore, the transition is reversible: if a DSC curve is plotted on cooling, an inverted cusp is obtained. It is possible, by suitable heat treatment, to partially crystallise a metallic glass and the fraction crystallised can be determined by DSC. Since the Curie temperatures of the crystalline phases are substantially above that of the glassy alloy [43], the magnitude of the specific heat anomaly at the Curie point of a partially crystallised alloy should be proportional to the fraction untransformed. This has been found to be the case for Metglas 2605 and a similar result has been obtained by Schowalter et al. [29].

The best confirmation that this is the Curie transition is provided, of course, by magnetic measurements. Five 100 mm lengths of Metglas 2605

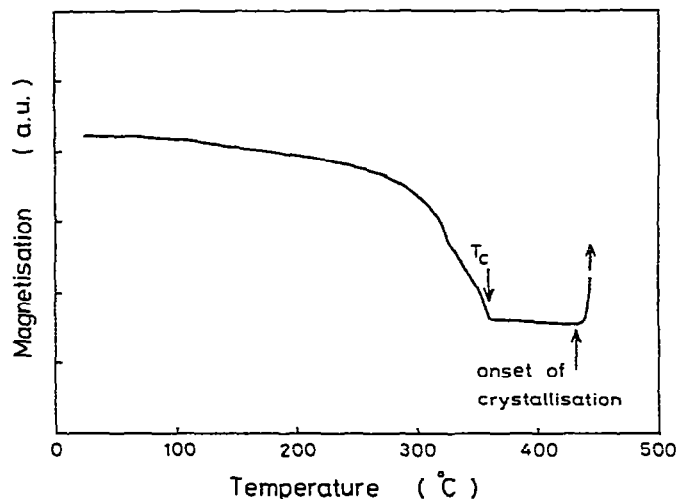


Fig. 13. Magnetisation (measured in arbitrary units) of as-received Metglas 2605 heated at approximately $200^{\circ}\text{C min}^{-1}$. The Curie point is marked.

ribbon were heated in a small tube furnace at about $200^{\circ}\text{C min}^{-1}$ and the magnetisation measured using an integrating fluxmeter. Figure 13 shows the result confirming that the effect being studied is the Curie transition.

The values of T_c corrected for temperature lag, obtained at different heating rates are given in Fig. 14. This shows clearly that there is a significant annealing effect during the determinations: at lower heating rates, the effect is greater and T_c is higher. Majumdar [32] made his magnetic measurements on Metglas 2605 at a heating rate of $100^{\circ}\text{C h}^{-1}$ (i.e. $1.67^{\circ}\text{C min}^{-1}$). His low-

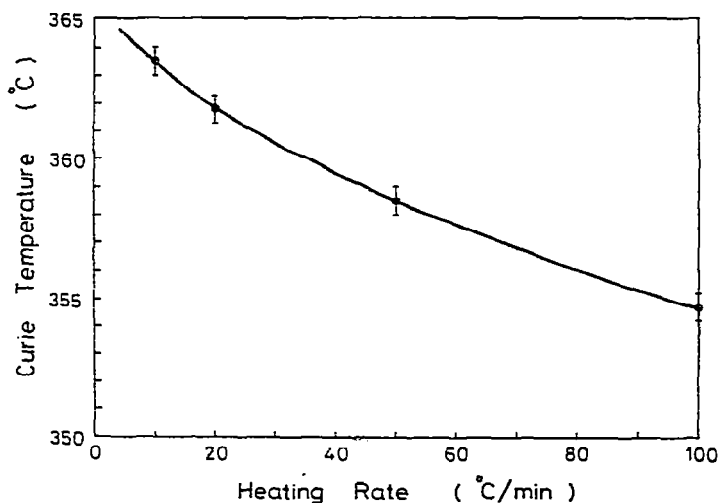


Fig. 14. The variation of Curie temperature as determined by DSC at different heating rates. The values have been corrected for temperature lag, so the observed variation shows the annealing effect on heating.

field susceptibility measurements gave a value for T_c of 359°C, whereas the maximum rate of change of magnetisation with temperature occurred at 364°C. These values cannot be compared directly with the DSC results in the present work, because these did not extend to such low heating rates, but the latter value of 364°C is in fair agreement with the expected value, ~365°C, from DSC (Fig. 14). It would be expected that the maximum specific heat would correspond to the maximum rate of change of magnetisation, and the agreement between the calorimetric and magnetic results helps to confirm the DSC temperature calibration. Majumdar [32] points out that his values do not agree well with that obtained by Hasegawa et al. [43] who give a value of 374°C. This value was obtained from magnetic measurements and required nine measurements of magnetisation in different fields at each of three temperatures near the Curie point. Thus in this case, the sample has spent more time at an elevated temperature. Majumdar claims the rise because of this is due to partial crystallisation, but it has been shown [44] that crystallisation has no effect on the T_c of the remaining glassy phase; the effect is due to a relaxation of the glassy phase.

It will be apparent that large discrepancies can arise in Curie point determinations because of this relaxation effect. For an alloy such as Metglas 2605, where T_c is quite high, the value which is determined is always distorted to some degree because of annealing during the determination. This dis-

TABLE 1

Details of the metallic glasses studied in this work

All materials were melt-spun.

Composition	Trade name †	Ribbon dimensions		As-quenched T_c (°C ± 0.2°C)
		Thickness ($\mu\text{m} \pm 2 \mu\text{m}$)	Width (mm ± 0.05 mm)	
$\text{Fe}_{80}\text{B}_{20}$	Metglas 2605 *	38	1.0	358.5
$\text{Fe}_{60}\text{Ni}_{40}\text{B}_{20}$ **		22	0.6	352.5
$\text{Fe}_{78}\text{Mo}_2\text{B}_{20}$	Metglas 2605A *	43	1.1	282.6
$\text{Fe}_{83}\text{P}_{12}\text{B}_5$ ***		23	1.0	320.8
$\text{Fe}_{40}\text{Ni}_{40}\text{P}_{14}\text{B}_6$	Metglas 2826 *	58	1.75	234.8

* From Allied Chemical Corp., Morristown, New Jersey, U.S.A.

** Kindly supplied by Dr. H.S. Chen of Bell Laboratories.

*** Prepared in our laboratory.

† Metallic glasses are now available commercially also from Vacuumschmelze GMBH, Hanau, W. Germany, under the trade name "Vitrovac", but none was used in the present work.

tortion is most severe for completely unrelaxed (i.e. as-received) samples. Of all the methods for determining T_c , the DSC method is the quickest and therefore involves the least distortion. For this reason, T_c measurements made by DSC can be used to study the relaxation in Metglas 2605 (Sect. 4). DSC is also a very convenient method and certainly more convenient than making all the magnetic measurements necessary for Arrott plots [43]. It has been shown above that, when the relaxation is taken into account, the agreement between the values of T_c determined by DSC and those determined by more sophisticated magnetic measurements is good.

The ease of determination of T_c by DSC depends on the magnitude of the specific heat anomaly at the Curie point. With Metglas 2605, there is no problem, but for metallic glasses with lower remanence, the cusp on the DSC curve is much smaller and the determinations of T_c may be less accurate.

The Curie temperatures of some metallic glasses, determined by heating at $50^\circ\text{C min}^{-1}$ and corrected for temperature lag, are given in Table 1. Evidently, the T_c is very composition-dependent (though it is always much below the values for the crystalline phases in these systems, e.g. $\alpha\text{-Fe}$: $T_c = 770^\circ\text{C}$; Fe_3B : $T_c = 520^\circ\text{C}$ [43]). In addition to the effect of composition, T_c can be affected by stress and by the configurational state (i.e. the degree of relaxation) of the glass. An externally applied hydrostatic compression causes a lowering of T_c [45]. Internal stresses (e.g. as induced by cold rolling) are, though, both tensile and compressive and therefore lead to an apparent smearing of the Curie transition, but not a shift [46]. The configurational dependence of T_c is indicated by the T_c changes on annealing, but it also means that materials produced at different cooling rates should have different values of T_c . This may account for the observation that as-quenched metallic glasses have more variable properties than when annealed. A variation in cooling rate during melt-spinning would give rise to a variation in properties, but on annealing, the range of initial structures would all tend to relax toward the same structure, so that the variability in properties would decrease. This was observed above for the T_c of $\text{Fe}_{80}\text{B}_{20}$ glass and by Hadnagy et al. [47] in their stress relaxation measurements on $\text{Fe}_{40}\text{Ni}_{40}\text{P}_{14}\text{B}_6$.

When a metallic glass is annealed, there may be relief of internal stresses, structural relaxation and crystallisation. (Separation into two amorphous phases is another possibility, but it has not been found in the glasses studied in this paper.) In general, the property changes on annealing reflect all these processes and may therefore not be convenient for studying just structural relaxation. For example, if coercive force, H_c , is measured, it is found to decrease because of stress relief and structural relaxation and it is difficult to separate the two effects [48]. Furthermore, H_c increases markedly once crystallisation starts. The measurement of Curie temperature, however, has particular advantages for investigating structural relaxation. Firstly, as outlined above, T_c is largely unaffected by stress relief [46]. Secondly,

it is affected by crystallisation only insofar as crystallisation causes the composition of the remaining amorphous phase to alter. (It is the T_c of the amorphous phase only which is measured.) In glasses undergoing eutectic crystallisation [49], the composition of the amorphous matrix remains unaltered during crystallisation. This is true of (at least) $\text{Fe}_{80}\text{B}_{20}$, $\text{Fe}_{40}\text{Ni}_{40}\text{B}_{20}$ and $\text{Fe}_{40}\text{Ni}_{40}\text{P}_{14}\text{B}_6$ of the glasses listed in Table 1. Thus, in these cases, the T_c changes correspond to structural relaxation and nothing else. The next section describes briefly how T_c measurements have been used to study the structural relaxation of $\text{Fe}_{80}\text{B}_{20}$ glass.

4. STRUCTURAL RELAXATION OF $\text{Fe}_{80}\text{B}_{20}$ GLASS

In all the work reviewed in this section, the Curie temperature measurements were made as described above, including corrections for temperature lag. The $\text{Fe}_{80}\text{B}_{20}$ glass used was Metglas 2605 ribbon from Allied Chemical Corporation. Short term (<3 h) heat treatments were performed in the DuPont calorimeter operating in isothermal mode. The constancy of the temperature during an anneal and the reproducibility were $\pm 0.5^\circ\text{C}$. For long term treatments, a tube furnace with an on/off temperature controller was used, the temperature being constant to $\pm 2.0^\circ\text{C}$. The correspondence between the temperature calibrations of the two heat treatment methods was checked. In DSC, some oxidation of the specimens occurred despite the purge gas in the cell: this was particularly so on annealing above 350°C , when the samples became straw-coloured. Oxidation in the tube furnace was prevented by sealing the specimens in Pyrex tubes under one third of an atmosphere of argon.

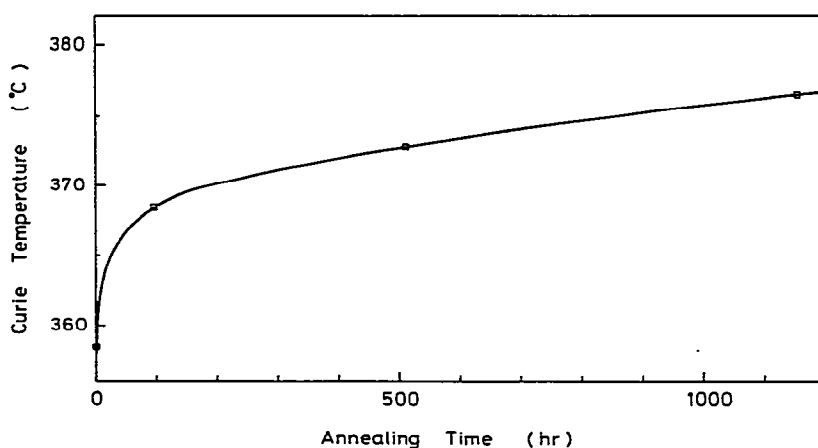


Fig. 15. The effect of annealing at 250°C on the Curie temperature of Metglas 2605: a rapid initial increase is followed by a slower rise.

Figure 15 shows the effect on the Curie temperature of annealing at 250°C. The general features of this curve, viz. that T_c rises at first rapidly and then more slowly, are the same over a wide range of annealing temperatures, but the process is much more rapid at higher temperature. T_c was still rising after 1000 h at 250°C, but it has been shown [44] that at higher temperatures T_c levels off in a reasonable time (e.g. 5 min at 400°C). The final value attained by T_c varies with annealing temperature, being lower at higher temperature [50,51]. The data from isothermal anneals have been used to construct Fig. 16, which is an isothermal transformation diagram for $\text{Fe}_{80}\text{B}_{20}$ glass. The diagram also contains crystallisation data and it can be seen that there is substantial structural relaxation before crystallisation. Such a diagram may be useful in extrapolating relaxation and crystallisation data to lower temperatures to see if either process is likely to be significant under service conditions. Its predictive value, however, is limited to simple isothermal anneals, whereas series of anneals at different temperatures are common in studying relaxation.

When the T_c levels off on annealing, it can be presumed that the glass is in internal equilibrium. This is supported by the fact that the same final value of T_c is attained whether the approach is from higher or lower values [46]. (The high starting value was attained by a pre-anneal at a lower temperature.) The approach from higher values is slower, as would be expected, since a glass with higher T_c values is in a more "relaxed" state, i.e. it has less free volume and lower atomic mobility [46]. It is possible to move reversibly between equilibrium states obtained on annealing at different temperatures [44]. At equilibrium, the T_c values uniquely specify the states of the glass,

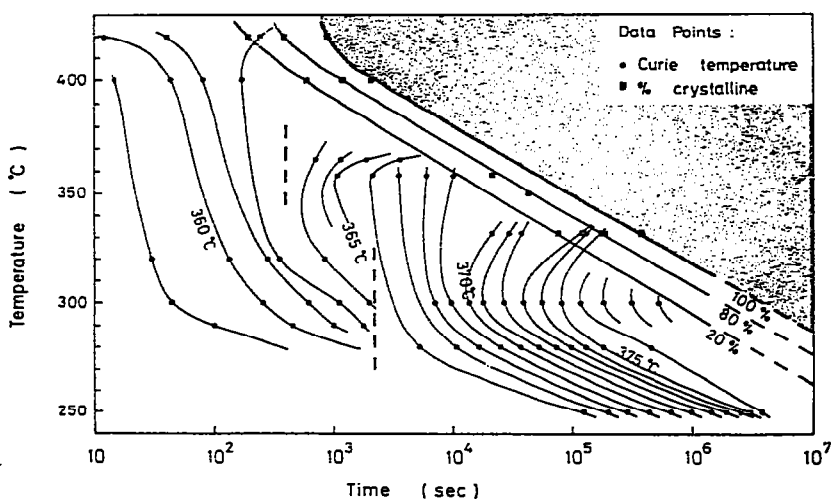


Fig. 16. Isothermal transformation diagram for Metglas 2605. The vertical broken lines separate data from DSC annealing and furnace annealing; the furnace was used for the longer times.

but this is not so away from equilibrium. In a "crossover" experiment, it has been shown that the same value of T_c can be obtained when the glass is not in equilibrium at the annealing temperature and again when it is, the value having departed appreciably in between [50].

The main conclusion from the above work is that the relaxation behaviour of $\text{Fe}_{80}\text{B}_{20}$ glass is very similar to that of oxide glasses [52] and polymers [53]. Thus metallic glasses appear to be true vitreous materials and the models developed to describe the relaxation of more conventional glasses [54,55] may be applicable to them. It should be noted, however, that while the precision of the T_c values is sufficient to justify a number of conclusions, the ratio of errors to changes in T_c in metallic glasses is greater than the corresponding ratio with, for example, the refractive index of oxide glasses, so that the metallic glass data will provide a less critical test of the models.

Annealing causes the T_c and the density of metallic glasses to increase [56], yet compression causes T_c to decrease [45]. Thus the structural change on annealing is not a simple densification (i.e. a uniform shortening of bond lengths); indeed, diffraction studies have shown that the bond lengths stay approximately constant [57]. The structural change causing the density increase and other property changes must be a change in topology involving an increase in the average co-ordination number of the atoms. Some insight on the atomic processes of relaxation may be gained by studying metallic glasses of different composition [46].

5. CONCLUSIONS

Metallic glasses with a high proportion of magnetic species are ferromagnetic and exhibit a sharp Curie transition. The Curie temperature, T_c , is a particularly good parameter for studying the structural relaxation of these materials, because, unlike other properties, it is unaffected by stress relief and, in some cases, is unaffected by partial crystallisation. The T_c can be measured rapidly using DSC and the reproducibility is good ($\pm 0.2^\circ\text{C}$) if the temperature lag of the sample is allowed for. A new method of determining the temperature lag in the DuPont DSC system has been developed and tested. In it, the lag is measured individually for each sample, without the need for weighing. The method requires no adaption of the basic instrument and is convenient in practice. The use of DSC to determine T_c is superior to other methods, not only because of its precision and convenience, but also because its speed minimises any annealing effects during the determination. The structural relaxation behaviour of metallic glasses, as studied by measuring their T_c , appears to be similar to that of more conventional glasses.

ACKNOWLEDGEMENTS

The work described above was carried out at the Department of Metallurgy and Materials Science, University of Cambridge. The author is indebted to the Northern Ireland Department of Education for financial support, to Professor R.W.K. Honeycombe for the provision of laboratory facilities, and to the Science Research Council for equipment. Helpful discussions with Dr. J.A. Leake and Dr. J.R. Saffell are gratefully acknowledged, as is the assistance of Dr. W. Howarth, who made the magnetic fluxmeter measurements. This paper was prepared during the tenure of a N.A.T.O. Research Fellowship at Harvard University.

APPENDIX: NICKEL SAMPLES

Sources and compositions of the nickel samples used for temperature calibration in DSC.

Nickel sponge

Source: Koch—Light Laboratories Limited

Specification: 0.001% total impurities

Nickel rod

Source: Johnson Matthey Chemicals Limited

Specification: Elements sought: Ag, Al, As, Au, B, Ba, Be, Bi, Ca, Cd, Ce, Co, Cr, Cs, Cu, Dy, Er, Eu, Fe, Ga, Gd, Ge, Hf, Hg, Ho, In, Ir, K, La, Li, Lu, Mg, Mn, Mo, Na, Nb, Nd, Ni, Os, P, Pb, Pd, Pr, Pt, Rb, Re, Rh, Ru, Sb, Sc, Se, Si, Sm, Sn, Sr, Ta, Tb, Te, Th, Ti, Tl, Tm, U, V, W, Y, Yb, Zn, Zr

Elements

detected: Iron 0.0015%, copper 0.0001%, aluminium, cadmium, chromium, magnesium, and silicon all less than 0.0001%

Carbonyl nickel pellets

Source: International Nickel Company Limited

Specification: 0.05% total impurities. Iron 0.01–0.04%, carbon 0.01–0.04%, and copper 0.005%

REFERENCES

- 1 T.R. Anantharaman and C. Suryanarayana, *J. Mater. Sci.*, 6 (1971) 1111.
- 2 H. Jones and C. Suryanarayana, *J. Mater. Sci.*, 8 (1973) 705.
- 3 R. Roy, *J. Non-Cryst. Solids*, 3 (1970) 33.
- 4 H.S. Chen and C.E. Miller, *Rev. Sci. Instrum.*, 41 (1970) 1237.
- 5 R. Pond and R. Maddin, *Trans. Metall. Soc. AIME*, 245 (1969) 2475.

- 6 H.S. Chen and C.E. Miller, *Mater. Res. Bull.*, 11 (1976) 49.
- 7 H.H. Liebermann and C.D. Graham, *IEEE Trans. Magn.*, MAG-12 (1976) 921.
- 8 H.S. Chen and D. Turnbull, *Acta Metall.*, 17 (1969) 1021.
- 9 S. Takayama, *J. Mater. Sci.*, 11 (1976) 164.
- 10 D.E. Polk and B.C. Giessen, in H.J. Leamy and J.J. Gilman (Eds.), *Metallic Glasses*, American Society for Metals, Metals Park, Ohio, 1978, p. 1.
- 11 R. Roy, B.C. Giessen and N.J. Grant, *Scr. Metall.*, 2 (1968) 357.
- 12 C.N.J. Wagner, *J. Non-Cryst. Solids*, 31 (1978) 1.
- 13 J.L. Finney, *Nature (London)*, 266 (1977) 309.
- 14 P.H. Gaskell, *J. Phys. C*, 12 (1979) 4337.
- 15 L.A. Davis, in H.J. Leamy and J.J. Gilman (Eds.), *Metallic Glasses*, American Society for Metals, Metals Park, Ohio, 1978, p. 190.
- 16 A.S. Argon, G.W. Hawkins and H.Y. Kuo, *J. Mater. Sci.*, 14 (1979) 1707.
- 17 M. Naka, K. Hashimoto and T. Masumoto, *J. Non-Cryst. Solids*, 28 (1978) 403; 29 (1978) 61.
- 18 R.A. Craven, C.C. Tsuei and R. Stephens, *Phys. Rev. B*, 17 (1978) 2206.
- 19 F.E. Luborsky, in E.R. Wohlfarth (Ed.), *Ferromagnetic Materials*, North Holland, Amsterdam, 1979.
- 20 M.G. Scott, in B. Cantor (Ed.), *Rapidly Quenched Metals III*, Vol. 1, Metals Society, London, 1978, p. 198.
- 21 P. Burroughs and M.G. Lofthouse, Application Brief TA 74, DuPont (U.K.) Ltd., Hitchin, England.
- 22 U. Köster and U. Herold, *Scr. Metall.*, 12 (1978) 75.
- 23 M.G. Scott, *J. Mater. Sci.*, 13 (1978) 291.
- 24 J.M.D. Coey, *J. Appl. Phys.*, 49 (1978) 1646.
- 25 A.I. Gubanov, *Fiz. Tverd. Tela (Leningrad)*, 2 (1960) 502.
- 26 T. Kaneyoshi, *J. Phys. Soc. Jpn.*, 45 (1978) 94.
- 27 H.S. Chen, R.C. Sherwood and E.M. Gyorgy, *IEEE Trans. Magn.*, MAG-13 (1977) 1538.
- 28 H.J. Leamy, E.M. Gyorgy, R.C. Sherwood, T. Wakiyama and H.S. Chen, *AIP Conf. Proc.*, 29 (1976) 211.
- 29 L.J. Schowalter, M.B. Salamon, C.C. Tsuei and R.A. Craven, *Solid State Commun.*, 24 (1977) 525.
- 30 S. Arajs, C.A. Moyer and K.W. Brown, *Phys. Scr.*, 17 (1978) 543.
- 31 P.J. Wojtowicz and M. Rayl, *Phys. Rev. Lett.*, 20 (1968) 1489.
- 32 A.K. Majumdar, *Solid State Commun.*, 29 (1979) 85.
- 33 H.S. Chen, R.C. Sherwood, H.J. Leamy and E.M. Gyorgy, *IEEE Trans. Magn.*, MAG-12 (1976) 933.
- 34 C.D. Graham, T. Egami, R.S. Williams and Y. Takei, *AIP Conf. Proc.*, 29 (1976) 218.
- 35 R.A. Baxter, in R.F. Schwenker and P.D. Garn (Eds.), *Thermal Analysis*, Vol. 1, Academic Press, New York, 1969, p. 65.
- 36 J.R. Saffell, *Thermochim. Acta*, 36 (1980) 251.
- 37 J.M. Barton, *Thermochim. Acta*, 20 (1977) 249.
- 38 A. Arrott, *Phys. Rev.*, 108 (1957) 1394.
- 39 R. Hultgren, P.D. Desai, D.T. Hawkins, M. Gleiser and K.K. Kelley, *Selected Values of the Thermodynamic Properties of the Elements*, American Society for Metals, Metals Park, Ohio, 1973, p. 353.
- 40 S.D. Norem, M.J. O'Neill and A.P. Gray, *Thermochim. Acta*, 1 (1970) 29.
- 41 H.W. Williams and B.L. Chamberland, *Anal. Chem.*, 41 (1969) 2084.
- 42 C. Sykes and H. Wilkinson, *Proc. Phys. Soc. London*, 50 (1938) 834.
- 43 R. Hasegawa, R.C. O'Handley and L.I. Mendelsohn, *AIP Conf. Proc.*, 34 (1976) 298.
- 44 A.L. Greer and J.A. Leake, in B. Cantor (Ed.), *Rapidly Quenched Metals III*, Vol. 1, Metals Society, London, 1978, p. 299.

- 45 T. Mizoguchi, AIP Conf. Proc., 34 (1976) 286.
- 46 A.L. Greer, M.R.J. Gibbs, J.A. Leake and J.E. Evetts, J. Non-Cryst. Solids, 38/39 (1980) 379.
- 47 T.D. Hadnagy, D.J. Krenitsky, D.G. Ast and C.-Y. Li, Scr. Metall., 12 (1978) 45.
- 48 M.R.J. Gibbs, J.E. Evetts and N.J. Shah, J. Appl. Phys., 50 (1979) 7642.
- 49 U. Herold and U. Köster, in B. Cantor (Ed.), Rapidly Quenched Metals III, Vol. 1, Metals Society, London, 1978, p. 281.
- 50 A.L. Greer and J.A. Leake, J. Non-Cryst. Solids, 33 (1979) 291.
- 51 J.A. Leake and A.L. Greer, J. Non-Cryst. Solids, 38/39 (1980) 735.
- 52 L. Boesch, A. Napolitano and P.B. Macedo, J. Am. Ceram. Soc., 53 (1970) 148.
- 53 A.J. Kovacs, J.M. Hutchinson and J.J. Aklonis, in P.H. Gaskell (Ed.), The Structure of Non-Crystalline Materials, Taylor and Francis, London, 1977, p. 153.
- 54 H.S.-Y. Hsieh, J. Mater. Sci., 13 (1978) 750.
- 55 O.S. Narayanaswamy, J. Am. Ceram. Soc., 61 (1978) 146.
- 56 H.H. Liebermann, C.D. Graham and P.J. Flanders, IEEE Trans. Magn., MAG-13 (1977) 1541.
- 57 T. Egami, J. Mater. Sci., 13 (1978) 2587.